Cell, Vol. 117, 483–494, May 14, 2004, Copyright ©2004 by Cell Press

Crystal Structure of the DegS Stress Sensor: How a PDZ Domain Recognizes Misfolded Protein and Activates a Protease

Corinna Wilken,[1] Karina Kitzing,[1] Robert Kurzbauer,[1] Michael Ehrmann,[2] and Tim Clausen[1,*]
[1]Institute for Molecular Pathology (IMP)
Dr. Bohrgasse 7
A-1030 Vienna
Austria
[2]Cardiff University
School of Biosciences
Museum Avenue
Cardiff CF10 3US
United Kingdom

Summary

Gram-negative bacteria respond to misfolded proteins in the cell envelope with the σE-driven expression of periplasmic proteases/chaperones. Activation of σE is controlled by a proteolytic cascade that is initiated by the DegS protease. DegS senses misfolded protein in the periplasm, undergoes autoactivation, and cleaves the antisigma factor RseA. Here, we present the crystal structures of three distinct states of DegS from *E. coli.* DegS alone exists in a catalytically inactive form. Binding of stress-signaling peptides to its PDZ domain induces a series of conformational changes that activates protease function. Backsoaking of crystals containing the DegS-activator complex revealed the presence of an active/inactive hybrid structure and demonstrated the reversibility of activation. Taken together, the structural data illustrate in molecular detail how DegS acts as a periplasmic stress sensor. Our results suggest a novel regulatory role for PDZ domains and unveil a novel mechanism of reversible protease activation.

Introduction

The fate of damaged proteins is determined by three major pathways, repair, degradation, and if the latter fail, aggregation. Aggregated proteins impose a severe stress on cells that can cause lethal damage, for example when an aggregated protein has an important function or when aggregates physically interfere with the integrity of cells. Several sophisticated quality control systems have evolved responding to protein folding stress. They include molecular chaperones and proteases, which selectively recognize proteins present in a nonnative state. Molecular chaperones either simply bind misfolded proteins to prevent aggregation or they actively assist in refolding. If refolding fails, irreversibly damaged proteins are degraded by proteases (Hengge and Bukau, 2003; Wickner et al., 1999). Because protein quality control is of vital importance, all cells have multiple stress response pathways that regulate this fundamental process. Compartment-specific signal transduction cascades detect misfolded proteins and transmit signals to dedicated transcription factors, which then adjust the levels of protein folding and degradation factors to the needs of the cell. In the cytoplasm, unfolded proteins are sensed by free pools of molecular chaperones (Liberek et al., 1992; Straus et al., 1990). Under normal conditions, the σ32 transcriptional activator is sequestered by the DnaK and DnaJ chaperones and targeted for degradation. Heat shock and other external stresses raise the amount of unfolded proteins, which preferentially interact with molecular chaperones thereby releasing σ32 to induce the heat shock response. In the extracytoplasmic stress response, the stress signal must cross a membrane, and thus more sophisticated pathways are required to transduce the signal from one compartment to another (Ma and Hendershot, 2001; Raivio and Silhavy, 2001). Despite the physiological importance of these pathways, little is known about the molecular mechanisms of stress sensing and transmembrane signaling.

A well-studied system is the σE envelope stress response that is triggered by excessive amounts of unfolded proteins, particularly unfolded outer membrane porins (Mecsas et al., 1993). The alternative σ-factor E (σE) is a transcriptional activator that directs the expression of genes encoding periplasmic chaperones, folding catalysts, and proteases, as well as genes involved in cell wall biogenesis (Rouviere et al., 1995). Under nonstress conditions, the activity of σE is inhibited by RseA, a membrane-spanning protein whose cytoplasmic domain is an anti-sigma factor that captures σE, thereby preventing σE from binding to RNA polymerase (Campbell et al., 2003; De Las Penas et al., 1997; Missiakas et al., 1997). Upon folding stress, RseA is degraded by a proteolytic cascade controlled by the membrane-anchored periplasmic protease DegS and the membrane-embedded metalloprotease YaeL (Ades et al., 1999; Alba et al., 2001, 2002; Kanehara et al., 2002). Ultimately, RseA digestion led to the release of active σE and the expression of stress genes (Ades et al., 2003). Recent evidence suggests that peptides corresponding to the C terminus of misfolded outer membrane proteins serve as stress signals that activate the protease activity of DegS by binding to its PDZ domains (Walsh et al., 2003). Thus, DegS seems to be the key player in the σE pathway acting as the periplasmic stress sensor as well as the initial activator of the proteolytic cascade (Young and Hartl, 2003). DegS is a member of the widely conserved HtrA family of oligomeric serine proteases. The defining feature of the over 180 family members is the combination of a catalytic domain (resembling the classical serine protease trypsin) and one or more C-terminal PDZ domains, which are well-known protein-protein interaction motifs (Harris and Lim, 2001; Harrison, 1996). Some, but not all, family members are classical heat shock proteins and are dealing with folding stress. They are typically localized in extracytoplasmic compartments such as the periplasm of Gram-negative bacteria, the ER and mitochondria of eukaryotes, the chloroplast of plants, or the extracellular space.

*Correspondence: clausen@imp.univie.ac.at

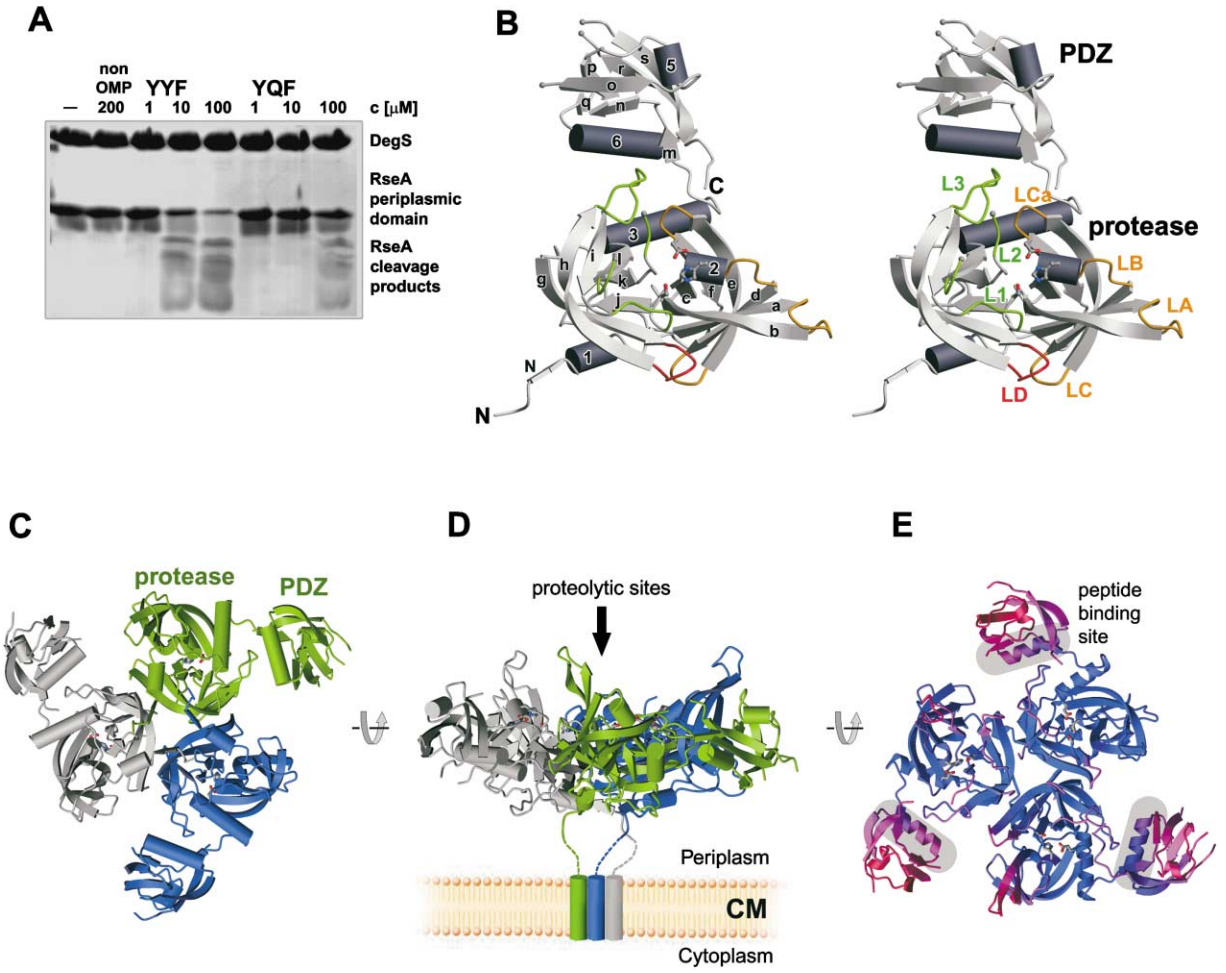

Figure 1. Structure of the *E. coli* DegS

(A) SDS-PAGE of RseA cleavage by DegS. The periplasmic domain of RseA was present in 30 μM, DegS in 10 μM, the YYF peptide (DNRLGLVYYF) and the YQF peptide (DNRLGLVYQF) in 1, 10, and 100 μM, respectively. The former peptide induced highest proteolytic activity, whereas the latter peptide was used to grow cocrystals with DegS. The reaction was stopped after 12 hr. In the control reactions, the assay was conducted without activating peptide and with a non-Omp peptide (EHLLVDFLQS).

(B) Stereo ribbon diagram of the monomer. All secondary structure elements (left) and active site loops (right) are labeled. The catalytic triad is shown as a stick model.

(C) Top view on the DegS trimer with each subunit colored differently.

(D) Side view of the trimer illustrating the relative orientation of DegS in the periplasm.

(E) Ribbon diagram of DegS, on which the thermal motion factors are mapped (blue: rigid parts, red: flexible parts). The location of the peptide-binding site of the PDZ domains is marked.

Here, we report the crystal structures of DegS alone and in complex with a peptide resembling the C-terminal tail of OmpC. The structural data provide the molecular framework for understanding how the PDZ domain of DegS perceives stress signals and how the proteolytic activity is reversibly activated by a series of conformational changes. In DegS, the PDZ domain offers a binding site for an allosteric activator, a so far unknown mechanism that seems to be conserved in related PDZ-proteases.

Results and Discussion

Structure of the DegS Monomer

To investigate the molecular mechanism of periplasmic stress sensing and activation of the σE response, we constructed and purified a DegS variant (residues 42–354) lacking its N-terminal membrane anchor. Truncated DegS was trimeric in solution, as judged by gel filtration and dynamic light scattering (data not shown), and retained proteolytic activity as shown by an in vitro cleavage assay (Figure 1A). Thus, the mutant should allow reconstruction of the biologically relevant structure. The structure of DegS was determined by molecular replacement using the protease domain of *E. coli* DegP (Krojer et al., 2002) as a search model and refined at 2.3 Å resolution.

Each subunit is 65 Å tall, 27 Å deep, and 38 Å wide (Figure 1B) and is composed of an N-terminal protease (residues 42–251) and a C-terminal PDZ domain (residues 252–354). The protease domain of DegS is similar to other proteases of the trypsin family consisting of

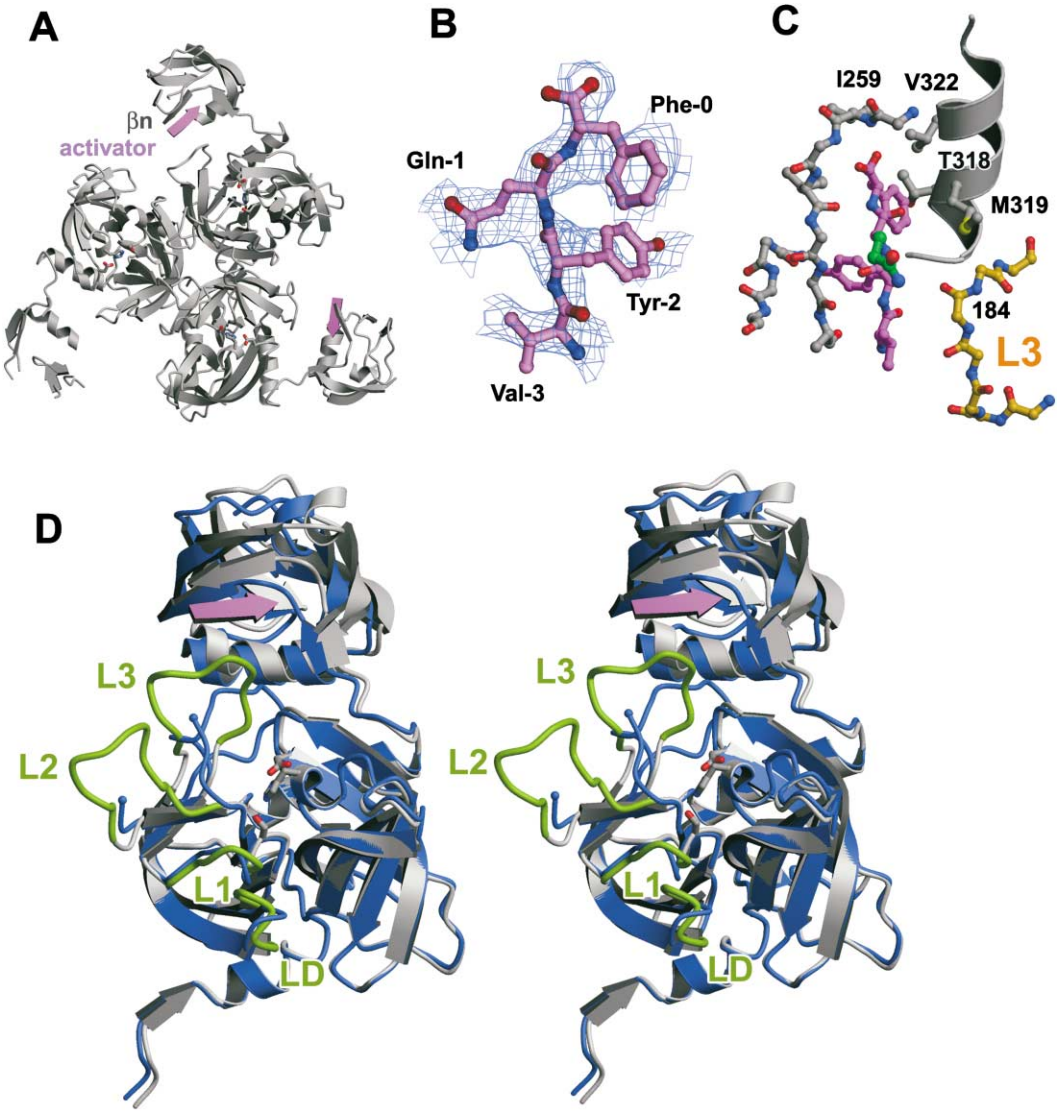

Figure 2. Peptide Binding to the PDZ Domain

(A) Stress-signaling peptides resembling the C terminus of OmpC (magenta) were bound to two of the three PDZ domains of DegS. They were bound in extended conformation as an additional β strand to βn.

(B) Electron density map showing the bound activator peptide. The Fo-Fc map was calculated prior to inclusion of the illustrated peptide in the model. The map was calculated at 2.4 Å resolution and is contoured at 2.5 σ.

(C) Binding of the activating peptide (magenta) involves residues from both PDZ (gray) and protease (orange) domains. The crucial residue to activate the protease, the Gln2, is highlighted in green.

(D) Stereo ribbon plot of the superimposed peptide-free (blue) and peptide-bound (gray) DegS. Some of the active site loops that rearrange upon activator binding are labeled (green).

two perpendicular β barrel lobes with a C-terminal helix (α3). Each of the antiparallel β barrels contains six strands (βa–βf, βg–βl) of identical topology, in which a Greek key motif (βa–βd, βg–βj) is followed by an antiparallel hairpin motif (βe–βf, βk–βl). The catalytic triad is located in the crevice between the two β barrels. The N-terminal barrel contributes two catalytic residues, His96 and Asp126, whereas the reactive Ser201 is part of the C-terminal barrel. One of the active site loops, L2 (loop nomenclature according to Perona and Craik [1995], see Figure 1B), was too flexible to be traced by electron density. In related proteases, L2 is directly involved in substrate binding, setting up the main chain binding patch and the S1 specificity pocket.

The overall structure of the PDZ domain of DegS is similar to other PDZ domains of bacterial origin (Krojer et al., 2002; Li et al., 2002; Liao et al., 2000) and contains seven β strands (βm–βs) and two α helices (α5, α6). The strands βn–βs form an antiparallel β sandwich, in which a two-stranded β sheet (βn, βo) is flanking a four-stranded β sheet (βq, βp, βr, βs). The short α helix 5 and its connecting loop cap one end of the β sandwich, while helix 6 caps the other end. As in other PDZ domains, a deep binding cleft for protein substrates can

be observed, which is mainly constructed by strand βn, its N-terminal loop (the so-called carboxylate-binding loop), and helix 6. The carboxylate-binding loop is formed by an Y-I-G-I motif (residues 258–261) that is homologous to the conserved G-L-G-F motif (Cabral et al., 1996). Two segments of the PDZ domain including residues 264–280 and 336–341 were not defined by electron density. In analogy to other members of the HtrA family, the former segment should contain an additional α helix (α4), whereas the latter segment should represent a β turn. A distinctive feature of the PDZ domain of DegS is a short C-terminal extension. Interestingly, this extension forms a two-stranded antiparallel β sheet with βm directing the C terminus back to the body of the protease. One of the terminal residues, Tyr351, packs into a shallow pocket of the protease domain undergoing van-der-Waals contacts with Leu124, Pro183, Arg256, and Tyr258. The C-terminal extension is further attached to the protease by a salt bridge between Glu350 and Arg253. Thus, the PDZ domain is tethered by a double linker to the protease domain.

The DegS Trimer Adopts a Funnel-Like Structure with Freely Accessible Proteolytic Sites

The crystalline asymmetric unit contains three DegS protomers assembled into a discrete trimeric particle. The protomers are packed symmetrically around a 3-fold molecular axis (Figure 1C), resulting in the burial of 4915 Å^2 of solvent-accessible surface. The trimeric particle obtains a funnel-like arrangement with the protease domains forming the core of the molecule and the PDZ domains extending outwards. The active sites of the protease are located on the concave side and are freely accessible. The three N termini that are connected to the membrane-anchoring helices protrude to the opposite side of the trimer, thereby fixing the orientation of DegS within the periplasm such that the funnel faces away from the cytoplasmic membrane (Figure 1D).

As in other HtrAs, formation of the trimer is exclusively mediated by the serine protease domains, in particular by residues of the N-terminal segment and of strands βg and βh. On the convex side of the funnel, a two-stranded β sheet (βg, βN*, the asterisk denotes the participation of the neighboring subunit) is formed between different subunits; this sheet is further stabilized by specific side chain interactions involving Ser46*, Asp153, and Ser208. In the center of the trimer, a large hydrophobic cluster is observed that is formed by residues Gly152, Ile151, Ile172, Tyr47*, Val51*, Leu156*, and Ile168*. The hydrophobic core is enclosed by an intersubunit hydrogen bonding network constructed by residues Gln48*, Ser174, Asp193, Asn197, and Glu230*. On the concave side of the funnel, the side chain of Leu164* is bound in a hydrophobic pocket of the molecular neighbor lined by residues Ile232, Phe234, and Pro229. Together, these interactions extensively stabilize the DegS trimer, an observation that is consistent with the stability of the trimer in solution. At low concentration, e.g., 1 μM, the monomeric form is undetectable as judged by gel filtration (data not shown).

Recent crystallographic models of other HtrAs indicated that the protease domains are forming the rigid part of the structure that is joined by a linker peptide to the highly mobile PDZ domain. The en-bloc mobility of the PDZ domains seems to be an essential mechanistic feature (Clausen et al., 2002). However, in DegS, the PDZ domain is tightly attached to the protease domain by an extended C terminus. Its peptide-binding groove is particularly well-defined as indicated by the crystallographic thermal motion factors (Figure 1E). It appears that a precise positioning of the PDZ domain is crucial for the function of DegS. Consistently, the overall root mean square deviation of the three DegS protomers is relatively low (0.78 Å), although the PDZ domains are not fixed by any crystal contacts.

The present crystal structure clearly contradicts the current model for the regulation of DegS activity. Based on the 3D structure of human HtrA2 (Li et al., 2002), it has been proposed that PDZ domains exert an inhibitory effect on the proteolytic activity of DegS by packing directly on the protease domain impeding access to the active site (Walsh et al., 2003). The DegS trimer, however, shows a rather open assembly of protease and PDZ domains; this assembly is stabilized by the C-terminal extension of the PDZ domain.

Binding of Stress-Signaling Peptides to the PDZ Domain Reveals a Novel Regulatory Function for a Protein-Protein Interaction Module

Peptides corresponding to C-terminal sequences of outer membrane proteins bind to the PDZ domain of DegS and function as activators (Walsh et al., 2003). Therefore, we tried to cocrystallize the protein with several peptides derived from C termini of outer membrane proteins varying in length (6 to 12 residues) and sequence. With one of these peptides (DNRLGLVYQF), which resembles the C terminus of OmpC (IVALGLVYQF) and stimulates proteolytic activity (Figure 1A), we obtained well-diffracting crystals. Although the peptide was bound to the rather flexible PDZ domain, its binding mode could be unequivocally determined.

As in other PDZ-peptide complexes (Doyle et al., 1996; Songyang et al., 1997), the signal peptide interacts with DegS in a β-augmentation process forming an additional β strand to βn–βo with the C terminus anchored by the carboxylate-binding loop (Figure 2A). There is only electron density for the four C-terminal residues of the peptide, suggesting that these residues are exclusively interacting with the PDZ domain (Figure 2B). Binding specificity is mainly conferred by the specific configuration of the 0, −2, and −3 binding pockets (Songyang et al., 1997), where pocket 0 anchors the side chain of the carboxy-terminal residue. In the DegS-activator complex, the phenylalanine in 0 position is bound in a hydrophobic pocket constructed by residues Ile259, Thr318, Met319, and Val322. By contrast, the side chain of the tyrosine residue at position −2 was not well defined by electron density. Presumably, this residue interacts with a main chain carbonyl of the PDZ domain. Most interestingly, the glutamine in −1 position interacts with the protease domain (Figure 2C). Its terminal amide nitrogen hydrogen bonds to the main chain carbonyl of Thr184, thereby pulling the flexible loop L3 15 Å away from its previous location. Furthermore, superposition of peptide-bound and peptide-free DegS indicated conformational changes of the distant active site loops L1, L2, and LD (Figure 2D). The most pronounced conformational changes are observed for loop L2. In the peptide-

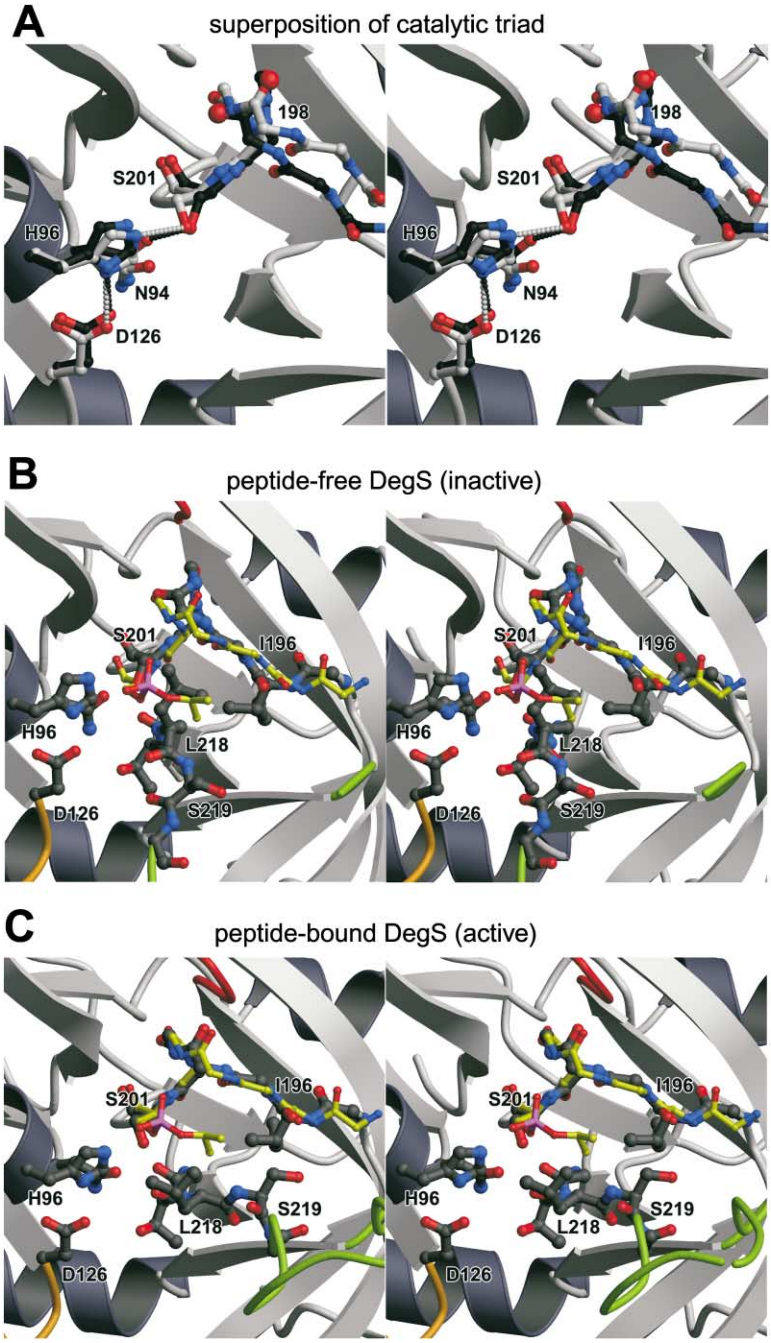

Figure 3. Architecture of the Proteolytic Site

(A) Alignment of the active site of peptide-bound (white) and peptide-free (black) DegS. The catalytic triad and the turn structure (residues 197–201) that sets up the oxyanion hole are shown in a ball-and-stick representation. The carbonyl oxygen of His198 that flips onto the other side of the peptide bond upon activation is highlighted. Hydrogen bonds are indicated by dotted lines.

(B) Stereo view of the proteolytic site of peptide-free DegS. Important active site residues are labeled, loop L2 is colored green, and loop LCa is colored orange. In order to illustrate location of the S1 specificity pocket, the structure is shown together with an aligned segment of the β-trypsin monoisopropylphosphoryl complex (yellow).

(C) Stereo view of the proteolytic site of peptide-bound DegS aligned with the same EI complex (yellow).

free form, the major part of this loop was highly flexible and not defined by electron density. Binding of the activator induces rearrangement of this loop, which in turn adopts a well-defined conformation.

Collectively, these results point to a novel mechanism of stress sensing and proteolytic activation, in which the PDZ domain acts as the key regulator. It detects unfolded proteins via specific C-terminal sequences that become accessible once the folding capacity of periplasmic chaperones is exceeded. These specific C-terminal tails have an YXF consensus motif (Walsh et al., 2003). The tyrosine and the phenylalanine fix the peptide to the PDZ domain, thereby bringing the −1 residue in proper position to interact with the protease. Therefore, in DegS, the PDZ domain is not a simple protein-binding domain. It attains a novel regulatory function being directly involved in intra- and intermolecular signaling. As discussed below, the PDZ domain represents a binding platform for an allosteric activator and thereby couples the binding of an unfolded protein with the activation of proteolytic activity.

Comparison of the Active Sites in the Peptide-Bound and Peptide-Free States

The DALI algorithm was employed to search for structural homologs of the protease domain and indicated that DegS is closely related to DegP (PDB code 1KY9, Z score 24.6), HtrA2 (1LCY, 21.7), epidermolytic toxin

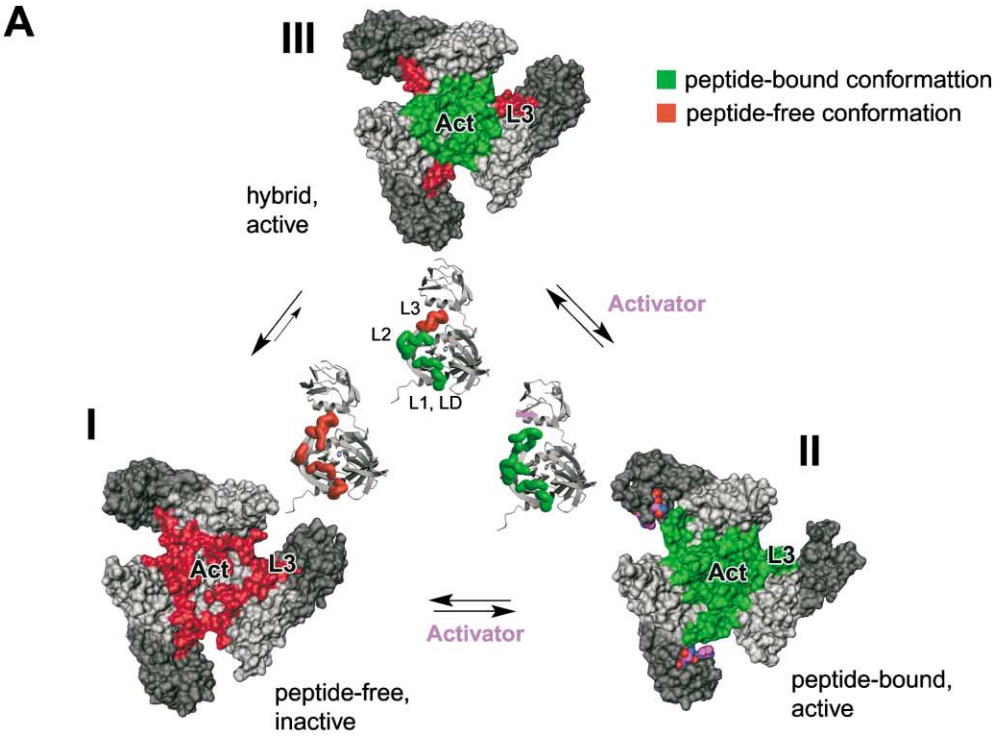
A
III
peptide-bound conformattion
peptide-free conformation
Act
L3
hybrid,
active
L3
L2
L1, LD
Activator
I
II
Act
L3
Act
L3
Activator
peptide-free,
inactive
peptide-bound,
active

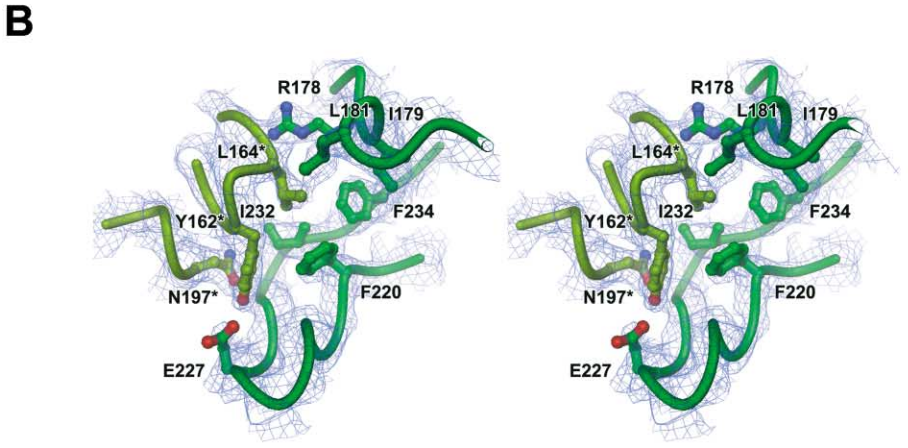
B
R178
L181
I179
L164*
Y162*
I232
F234
N197*
F220
E227
R178
L181
I179
L164*
Y162*
I232
F234
N197*
F220
E227

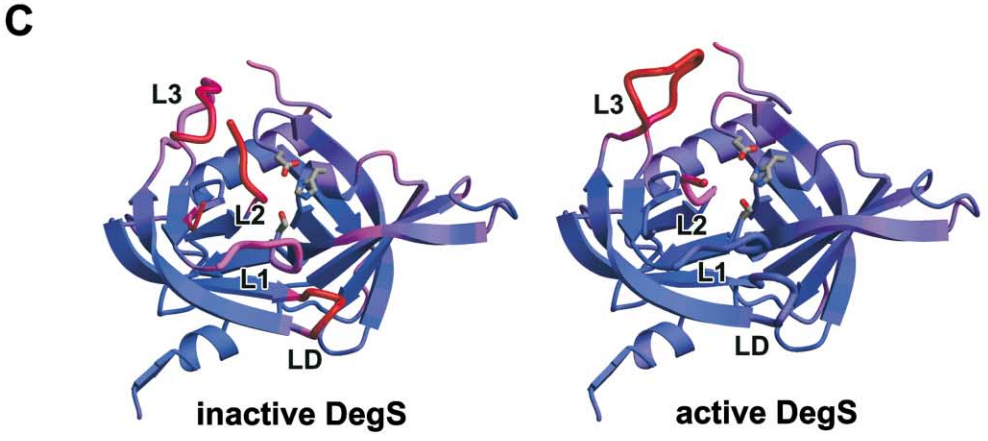
C
L3
L2
L1
LD
inactive DegS
L3
L2
L1
LD
active DegS

(1AGJ, 15.5), and β-trypsin (5PTP, 14.1). The multiple structural alignment of these enzymes allows the following mechanistic conclusions:

(1) In the mechanism for classic serine proteases, a tetrahedral oxyanion intermediate is formed during catalysis, which is favorably stabilized by a structural feature known as "oxyanion hole." In the trypsin family, the NH groups of Gly193 and Ser195, one of the residues of the catalytic triad, build this pocket. In peptide-free DegS, the corresponding 198–201 backbone adopts a similar turn structure, but the CO bond of His198 points into the wrong direction, i.e., into the catalytic pocket, abolishing stabilization of the oxyanion intermediate (Figure 3A). Furthermore, the fine-tuned serine-histidine interplay of the catalytic triad seems to be severely disturbed. The hydroxyl group of Ser201 interacts with Asn94 and is not activated by His96 for the committing nucleophilic attack. In the peptide-bound form, His198-CO flips onto the opposite side of the protein backbone, allowing formation of a proper oxyanion hole. Furthermore, a functional catalytic triad is now established by Ser201, His96, and Asp126.

(2) The S1 pocket primarily determines the substrate specificity of individual serine proteases. In the peptide-free form, the S1 specificity pocket is blocked by Leu218, as illustrated by the alignment with an EI complex of β-trypsin (Figure 3B). In peptide-bound DegS, a well-defined hydrophobic S1 pocket can be observed that is formed by Ile196, Leu218, and Ser219 (Figure 3C). The P1 side chain of a substrate should adopt a similar orientation as the propyl group of the aligned β-trypsin monoisopropylphosphoryl derivative. Thus, the S1 specificity pocket of DegS seems to be well suited to accommodate small hydrophobic residues. This finding is consistent with the reported substrate selectivity (Walsh et al., 2003). In the native substrate, RseA, cleavage occurs at a single peptide bond between Val148 and Ser149. However, even a strict S1 selectivity cannot explain the remarkable substrate specificity of DegS. Due to the topology of RseA, which is like DegS a type I transmembrane protein, it can be speculated that the scissile bond of RseA has to be part of an extended, unstructured region of about 30 residues that has to find its way from the membrane-facing side of DegS to the opposite surface, where the active sites are located. The structure indicates that the substrate has not to reach over the edge of the trimeric funnel. There is a cleft between protease and PDZ domain that offers a shortcut to the active site (Figure 1). It is tempting to speculate that this cleft employs further geometric and electrostatic constraints to a potential substrate and thus might function as a molecular ruler to identify RseA.

(3) Normally, the N-terminal residues of loop L2 act as a template to which protein ligands bind via their main chain atoms forming a short stretch of an antiparallel β sheet. Only the corresponding segment of peptide-bound DegS (residues 217–219) obtains a conformation that would allow main chain binding. Interestingly, the hinge residue for the reorientation of loop L2, Leu218, is part of this binding patch.

Taken together, our data clearly demonstrate that the proteolytic site of peptide-free DegS exists in an inactive state, in which substrate binding as well as catalysis are prevented, whereas the peptide-bound form has a functional proteolytic site. During activation, loops L1, L2, and LD undergo conformational changes that are triggered by binding of the activator to the PDZ domain. The structural flexibility of the corresponding loops in the inactive form, expressed by their elevated thermal motion factors (73.8 $Å^2$ compared to 41.2 $Å^2$ of the protease domain), is a prerequisite for this transition.

Reversible Protease Activation Mediated by a PDZ Domain

Peptide binding to DegS generated an asymmetric trimeric particle, in which one of the PDZ domains was less ordered than the others. Although interpretation of the electron density map of this PDZ domain was rather difficult, a bound activating peptide could not be identified, suggesting that the peptide-binding site is not or only partially occupied. This difference might be due to a distinct conformation of loop L3, which was slightly bent away from the PDZ domain. In contrast, the active site loops L1, L2, and LD obtain similar folds in all three subunits, thereby forming three functional proteolytic sites. To further investigate the asymmetric properties of peptide-bound DegS, we incubated crystals of the activator complex for 30 min in an activator-free solution. The structure obtained from these backsoaked crystals clearly indicated the release of the activating peptide with the concomitant reorientation of activator-binding loop L3 into its "peptide-free" conformation. By contrast, the active site loops L1, L2, and LD were still present in their active conformation. Due to the hybrid nature of this structure, we believe that it could represent an intermediate of the transition from active to inactive DegS. Interestingly, extensive backsoaking for 12 hr restored the inactive state of DegS, showing the reversibility of the transition (Figure 4A).

The DegS activation cycle represents a novel mecha-

Figure 4. Reversible Activation of DegS

(A) The present structural data allow the description of three different states I, II, and III, which are defined by the conformation of the activation domain (Act: loops L1/L2/LD) and of loop L3. The molecular surfaces of the respective trimers are represented using a specific color code for the defining structural elements (red: peptide-free, green: peptide-bound conformation). The corresponding protomers are shown in a ribbon presentation. Structure III represents a hybrid structure with the activation domain in its active and loop L3 in its inactive conformation.

(B) Stereo plot showing the active state of the activation domain with the newly formed interactions between loops L3/L2 of one subunit (green) and L1*/LD* of the molecular neighbor (light green). The model is shown together with the final 2Fo-Fc electron density map calculated at 2.4 Å resolution and contoured at 1.2 σ.

(C) The ribbon plot shows the protease domain of DegS with mapped thermal motion factors (blue: rigid parts, red: flexible parts). The relevant active site loops are labeled. Note that only loops comprising the activation domain (L1, L2, LD) become more rigid, whereas loop L3 is still flexible. The average B values for the protease domain, LD, L1, L2, L3 are 41.2, 87.3, 70.9, n.d., 69.3 for the uncomplexed and 71.3, 61.0, 58.6, 110.5, 128.1 for the active form, respectively.

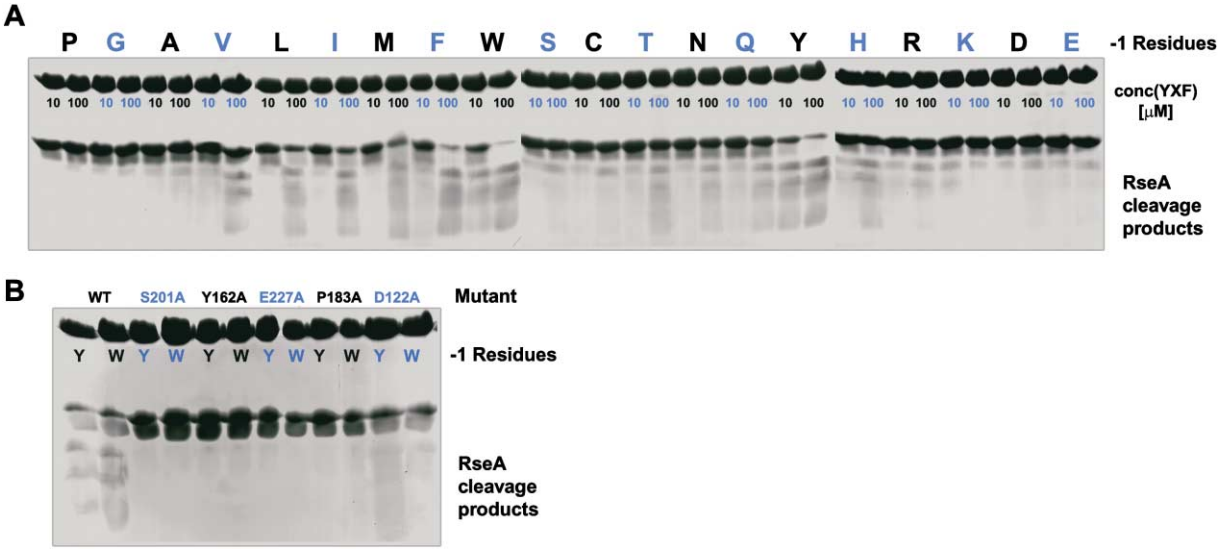

Figure 5. Biochemical and Mutational Analyses of the DegS Activation Mechanism

(A) SDS-PAGE of the cleavage reaction, in which the periplasmic domain of RseA (30 μM) was incubated with DegS (10 μM) for 12 hr. To test the importance of the penultimate residue of the activating peptide, 20 different derivatives of the DNRLGLVYXF peptide were synthesized varying in the X position and added to the reaction. Final activator concentrations of 10 and 100 μM were optimal to rank the individual activation potentials.

(B) Analysis of different DegS mutants using the RseA cleavage reaction. The assays were carried out for 12 hr using with different YXF peptides. Illustrated are the assays with the YYF (100 μM) and YWF (100 μM) activators.

nism that bears some similarities to the classical trypsin activation. In trypsin, transition from the inactive to an active state is achieved by reorientation of the so-called "activation domain," which is formed by loops L1, L2, and LD (Huber and Bode, 1978). The structure of the inactive/active hybrid suggests that DegS has an identical activation domain. In activated DegS, stabilization of the activation domain is achieved by a multitude of hydrophobic and polar interactions: Loops L1, L2, and LD rearrange such that a novel hydrophobic cluster is formed by residues Ile179, Leu181, Phe220, Ile232, Phe234, Tyr162*, and Leu164* (Figure 4B). The active conformation of loops L3 and LD* is further stabilized by two hydrogen bonds that are formed between the guanidino group of Arg178 and the two main chain carbonyls of Leu164* and Gln166*. Furthermore, Tyr162* forms a short-distance hydrogen bond with Glu227, thereby defining the conformation of the previously highly flexible loop L2. In addition, Tyr162* interacts with the side chain of Asn197* that turns around and further fixes L2 by binding to the main chain amide of Glu230. Ultimately, the rearranged activation loop LD* seems to induce a peptide flip in loop L1* that is required to form the oxyanion hole and the catalytic triad. This step is provoked by formation of a hydrogen bond between the backbone carbonyl of His198* and the amide nitrogen of Tyr162*.

Remarkably, classical trypsin proteases and DegS use different activation signals. In trypsin, binding of a hydrophobic N terminus into the so-called "Ile16 pocket" causes rearrangement of the activation domain. This process is either triggered by propeptide cleavage (Huber and Bode, 1978) or by the action of *trans*-acting protease activators (Bode and Huber, 1976; Friedrich et al., 2003). By contrast, in DegS, peptide binding to the PDZ domain causes reorientation of the activation domain. A key player in this mechanism is loop L3 that transduces the signal from the PDZ to the protease domain. Another similarity to trypsin activation is a disorder-order transition. In the inactive trypsinogen, the activation domain is highly flexible, whereas in the active trypsin protease it occupies a well-defined position poised for catalysis. Analogously, the activation domain of DegS becomes more rigid upon allosteric activation (Figure 4C). The remarkable difference to classical proteases is that activation of DegS is reversible, guaranteeing an immediate and flexible cellular response toward folding stress.

Biochemical and Mutational Analysis of the DegS Activation Mechanism

The structure of the DegS-activator complex suggests that the X residue of YXF C-terminal peptides interacts directly with the protease domain and is involved in regulation of activity. The side chain of this X residue should contain a hydrogen donor group in order to contact loop L3 and to promote allosteric activation. To test this proposal in vitro, we synthesized different decapeptides containing the consensus sequence DNRLGL VYXF with X being any of the 20 bioactive amino acids. Surprisingly, the selectivity for the −1 residue was rather weak. Only small amino acids (Pro, Gly, Ala, Ser, and Cys) and the negatively charged aspartate and glutamate failed to stimulate DegS (Figure 5A). The most pronounced activation was achieved with aromatic residues in −1 position (Phe, Tyr, and Trp) with the Tyr derivative being the most activating peptide. The remaining residues (Val, Leu, Ile, Met, Thr, Asn, Gln, His, Lys, Arg) lead to moderate activation. These results suggest the following hypotheses: (1) Regarding activation,

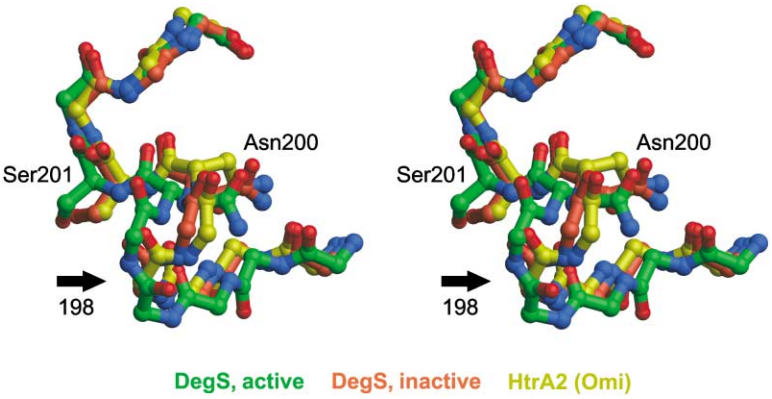

Figure 6. Comparison of DegS and HtrA2 (Omi)

The stereo picture shows an alignment of active DegS (green), inactive DegS (red), and HtrA2 (yellow). The chosen segment comprises DegS residues 195–204 (HtrA2 167–176), which include the active site serine and loop L1 that forms the oxyanion hole. Key residues are indicated as well as the 198 peptide that is important for DegS activation. Notably, the L1 backbone of HtrA2 has a similar turn structure as the inactive DegS.

DegS seems to exhibit a clear preference for bulky −1 side chains, which might reflect the steric limitations of loop L3 to approach the PDZ domain. (2) Both hydrophobic and polar residues appear to be capable to induce conformational rearrangement of loop L3, most probably by different kinds of interactions. Peptides carrying a hydrogen donor group in −1 position should follow the mechanism of the structurally characterized YQF peptide and hydrogen bond to loop L3. Hydrophobic −1 residues have to employ an alternative mechanism. These residues could undergo positive van-der-Waals contacts with loop L3, thereby stabilizing its active conformation, which in turn should establish a functional proteolytic site in an equivalent manner as observed for the YQF peptide. Mutational analyses support this idea (Figure 5B). Taken together, the structural and biochemical evidence suggests that the contact between the activator −1 residue and loop L3 is crucial for propagating the switch signal from the PDZ to the protease domain.

To further validate the proposed activation model, we mutagenized key residues of the mechanistic important loops LD, L1, L2, and L3 and analyzed the resulting variants using purified protein in the protease activation assay. In all cases, structural integrity was verified by gel filtration chromatography and dynamic light scattering (data not shown). As expected, replacement of the active site Ser201, one of the residues of the catalytic triad, by alanine completely abolished proteolytic activity (Figure 5B). Thus the S201A mutant was chosen as a reference to judge the effect of the other exchanges. As discussed previously, Tyr162 and Glu227, residues of loops LD and L2, respectively, are critical to stabilize the active conformation of the activation domain. Consistently, changing Tyr162 and Glu227 to Ala had an equally severe effect as replacing the central nucleophile Ser201,

Table 1. Data Collection and Model Refinement

	Structure I: Peptide-Free	Structure II: Peptide-Bound	Structure III: Intermediate
Data Collection			
Unit cell	C2	C2	C2
Cell constants	a = 207.7 Å	a = 206.0 Å	a = 207.0 Å
	b = 143.1 Å	b = 142.7 Å	b = 142.7 Å
	c = 41.5 Å	c = 41.2 Å	c = 41.2 Å
	β = 90.1°	β = 89.2°	β = 90.0°
Resolution (Å)[a]	15–2.30 (2.34–2.30)	15–2.40 (2.44–2.40)	20–3.05 (3.16–3.05)
Measured reflections	99,437 (5042)	72,161 (3741)	37,632 (3147)
Unique reflections	51,588 (2613)	42,509 (2223)	21,157 (1992)
Data redundancy	1.93 (1.93)	1.70 (1.68)	1.78 (1.59)
I/sig I	24.1 (2.4)	16.2 (1.2)	7.6 (1.3)
Data completeness (%)	96.5 (99.5)	91.8 (94.7)	93.5 (87.6)
R_{sym} (%)[b]	4.9 (20.5)	6.2 (58.0)	6.9 (44.6)
Refinement			
R_{cryst}/R_{free} (%)[c]	19.8/24.8	21.3/27.2	23.6/29.7
Protein atoms	6289	5964	6387
Ligand atoms	—	80	—
Solvent atoms	330	224	—
Rmsd bond length (Å)	0.012	0.011	0.010
Rmsd bond angles (°)	1.59	1.66	1.47
Rmsd B-factors (Å²)	4.54	4.55	2.91

[a] Numbers for last resolution shell are given in parenthesis.

[b] R_{sym} is the unweighted R value on I between symmetry mates.

[c] $R_{cryst} = \Sigma_{hkl}||F_{obs}(hkl)| - k|F_{calc}(hkl)||/\Sigma_{hkl}|F_{obs}(hkl)|$ for the working set of reflections; R_{free} is the R value for 5% of the reflections excluded from refinement.

demonstrating the crucial importance of these residues. Furthermore, we mutagenized Pro183, a residue located in the central region of loop L3, to examine the steric restraints imposed on this loop. The failure of the YYF peptide to activate the P183A mutant suggests that loop L3 has to acquire a specific conformation to promote contact with the activator. Together with the results from the amino acid screen, this finding implies that transferring the switch signal from the PDZ to the protease domain is a sterically demanding task. Thus it appears plausible that the position of the PDZ domain has to be tightly and precisely fixed. Several interdomain salt bridges determine the orientation of the PDZ domain, one of which (Arg256 with Asp122) is conserved in all DegS homologs. Consistent with this idea, the D122A mutant displayed reduced proteolytic activity upon YYF activation. The residual activity of this mutant might be attributed to the fact that the PDZ domain is tethered by multiple interactions to the protease body and that deletion of a single salt bridge causes only an incomplete domain reorientation. Remarkably, the D122A mutant eluted differently from the NiNta column compared to all other DegS variants. This observation might also suggest an altered position of the PDZ domain that carries the C-terminal His-tag. Taken together, the mutational analysis supports the proposed model of how DegS can be allosterically activated. The presented mutations also abolished stimulation by other YXF peptides, as shown for example for the YWF peptide in Figure 5B, and thus a common mechanism of activation can be anticipated.

Implications for Other PDZ-Proteases

DegS belongs to the superfamily of PDZ-proteases. Its members include DegP, DegQ, Tsp, YaeL, and HtrA2, which play crucial roles in establishing protein quality control. Although their protease domains belong to different classes, they share a homologous PDZ domain that might regulate protease activity. The HtrA proteases constitute the largest subfamily of PDZ-proteases, including several well-characterized proteins. Human HtrA1 is essential for progression and invasion of several cancers (Baldi et al., 2002; Shridhar et al., 2002), HtrA2 is crucial for apopotosis (Hegde et al., 2002; Jones et al., 2003; Martins et al., 2002; Srinivasula et al., 2003; Yamaguchi et al., 2003; Yang et al., 2003), and HtrA3 is involved in pregnancy (Nie et al., 2003). Furthermore, bacterial DegP and DegS are essential for survival under protein folding stress caused by hostile environments. These proteins are also essential for many pathogens, which become exposed to the immune system (Pallen and Wren, 1997). It is therefore apparent that the novel mechanisms of reversible protease activation and recruitment of PDZ domains for stress sensing and autoactivation represent key regulatory events determining cell fate.

Recent evidence suggests that the activity of all HtrA proteases can be reversibly switched on or off and that the relevant mechanism including regulatory PDZ domains is conserved. Human HtrA2 (Omi) performs a crucial role in apoptosis, promoting caspase-dependent and caspase-independent cell death. However, the molecular details of regulation of HtrA2 are still elusive. Structural comparison of DegS and HtrA2 clearly indicates that the active site of HtrA2 is present in a nonfunctional state. There is no oxyanion hole and most likely no proper catalytic triad. Consistently, some active site loops of HtrA2 align better to the inactive than to the active form of DegS (Figure 6). It was shown recently that binding of specific peptides to the PDZ domain of HtrA2 resulted in a marked increase in proteolytic activity (Martins et al., 2003). Since the position of the PDZ domain in the HtrA2 crystal structure was strongly influenced by crystal packing constraints, we believe that in solution, the PDZ domain of HtrA2 might function similarly as in DegS, trapping the flexible loop L3. Upon a proper stimulus, the PDZ domain might reorient, thereby releasing L3, which in turn triggers adjustment of the activation domain yielding a functional active site. In the reported PDZ deletion mutant, which exhibited increased proteolytic activity (Li et al., 2002; Martins et al., 2003), loop L3 probably cannot be fixed in the domain interface and thus activates the protease. Interestingly, the DegP protein seems to also employ a similar mechanism. In its chaperone conformation, the DegP protease was observed in a completely inactive state. Activation should require larger conformational changes than in DegS since the active site loops L1 and L2 are severely distorted and attain different conformations. For example the turn structure of loop L1 that sets up the oxyanion hole is preformed in DegS and HtrA2, while it is entirely absent in DegP (see also Figure 6 in Clausen et al., 2002). However, DegP can be allosterically activated by specific peptides that bind to its PDZ domains (Jones et al., 2002) and has a flexible loop L3 that is wedged between protease and PDZ domains (Kim et al., 2003; Krojer et al., 2002). This mechanistic conservation implies that DegS sets the stage to better understand the regulation of proteases containing PDZ domains.

Experimental Procedures

Cloning, Expression, and Protein Purification

The open reading frame encoding the protease and PDZ domain (residues 43–354) of *E. coli* DegS was PCR amplified from the genome of strain DH5α. The PCR product was digested with NdeI and XhoI and cloned into pET-15b. This construct expresses the recombinant protein with a C-terminal His-tag. The plasmid was transformed into the *E. coli* strain BL21(DE3). Cells were grown at 37°C in LB medium. At OD_{600} = 0.6, overexpression was induced with 1 mM IPTG for 3 hr. Cells were harvested by centrifugation and lysed by sonication in 50 mM sodium phosphate buffer (pH 7.5) and 200 mM NaCl on ice. The protein was purified using Ni-NTA resin (Qiagen) and a Superdex 200 column in 10 mM sodium phosphate buffer (pH 7.5) and 200 mM NaCl. The protein was >99% pure and monodisperse as judged by SDS-PAGE and dynamic light scattering (DynaPro, Protein Solutions), respectively. Prior to crystallization, the protein buffer was exchanged by a NAP10 desalting column (Pharmacia) to 10 mM sodium phosphate (pH 7.5). Finally, the protein sample was concentrated to 16 mg/ml by ultrafiltration (Centriprep-10, Amicon). Se-Met-labeled DegS was overexpressed from the *met*$^-$ *E. coli* strain B834(DE3). All mutants of DegS were constructed using a QuickChange TM Site-Directed Mutagenesis Kit (Stratagene) and verified by sequencing. They were purified and assayed for RseA cleavage under the same conditions as the wild-type protein (see below).

Crystallization

Crystallization was carried out at 19°C using the sitting drop vapor diffusion method. Although crystals of the DegS protein grew in the

first screening round, extensive optimization of initial crystallization conditions was required. The keys for obtaining well-diffracting crystals were a phosphate-buffered protein solution and the use of $MgCl_2$ as crystallization additive. Crystals of DegS were grown in sitting drops at 19°C by mixing 4 μl of protein with 2 μl of a crystallization solution containing 0.1 M HEPES (pH 7.5), 6% PEG 6000, 9% MPD, and 10 mM $MgCl_2$. Crystal trials were setup in cryschem plates with a reservoir volume of 400 μl. Monoclinic crystals appeared after 3 days with dimensions of 100 × 50 × 400 μm^3. For cryo measurements, crystals were transferred from the crystallization drop to the mother liquor supplied with 18% MPD as cryoprotectant and rapidly frozen in a 100 K stream of nitrogen gas. For crystallization of the DegS-activator complex, the peptide DNRLGLVYQF was added to DegS protein (final concentration of the peptide was 100 μM) and incubated 30 min before setting up the cocrystallization trials. Cocrystals containing the DegS-activator complex appeared within a few days under the same conditions as for the free protein. In another experiment, the cocrystals were incubated for 30 min or 12 hr in an activator-free solution.

Structure Determination and Refinement

High resolution data of the SeMet-substituted protein and the activator complex were collected at the ESRF synchrotron, at beamline ID14-4 (λ = 0.9393 Å) using a Q4R ADSC CCD detector. Backsoaked crystals were analyzed in-house on a MarResearch image plate. Data were integrated using DENZO and scaled with SCALEPACK (Otwinowski and Minor, 1997). All crystals were of the monoclinic space group C2 with one DegS trimer in the asymmetric unit. The structure of the uncomplexed protein was determined by molecular replacement using the program MOLREP of the CCP4 package (CCP4, 2002) and the protease domain (residues 11–259) of *E. coli* DegP (Protein Data Bank ID 1KY9) as a search model. Electron density maps based on the coefficients 2Fo-Fc and 3Fo-2Fc were calculated from the phases of the initial model. The resulting maps were used to build atomic models in O (Jones et al., 1991). Refinement, model rebuilding and water incorporation proceeded smoothly via rigid body, positional, and later B factor optimization in CNS (Brunger et al., 1998). The entire structure was checked using simulated annealing composite omit maps. Some protein segments including residues 221–229, 264–280, and 336–341 were hardly visible in these maps and were therefore omitted from the model. The refined DegS structure was used to solve the structures of the activator complex and the backsoaked crystal form. During refinement of the activated DegS, clear electron density developed for two activator molecules within the trimeric protein. In contrast to ligand-free DegS, the entire protease domain was well defined, whereas one of the PDZ domains exhibited an increased flexibility allowing only building its peptide-binding groove. Refinement of the backsoaked form revealed a hybrid structure of the peptide-bound and peptide-free DegS. Similarly to uncomplexed DegS, the latter two structures were validated by omit electron density maps. Especially the proteolytic site that underwent pronounced conformational remodeling was carefully inspected. Corresponding omit electron density maps and maps calculated at lower resolution unequivocally revealed the conformational changes yielding a functional proteolytic site. The strongly decreased thermal motion factors of the contributing amino acid stretches further validated the relevance of the observed changes. The data collection and refinement parameters are summarized in Table 1. All graphical presentations were prepared using the programs MOLSCRIPT (Kraulis, 1991), RASTER3D (Merritt and Bacon, 1997), and DINO (http://www.dino3d.org).

In Vitro Cleavage Assay

Proteolytic activity was measured by following cleavage of the RseA antisigma factor. The periplasmic domain of *E. coli* RseA (residues 121–216) was overexpressed at 37°C as an N-terminal His-tag protein using the pET15b vector. The soluble protein was purified by NiNTA affinity chromatography and concentrated to 7.5 mg/ml in a buffer containing 50 mM phosphate (pH 7.5). Cleavage assays were performed at 37°C in 100 mM sodium phosphate (pH 7.5), 200 mM NaCl, 10% glycerol, 5 mM $MgCl_2$, and 1 mM DTT. The reaction was stopped by adding SDS sample buffer and boiling. The samples were analyzed by SDS-PAGE.

Acknowledgments

The authors wish to thank Joanne McCarthy for excellent assistance during data collection at beamline ID14-4 (ESRF, Grenoble). We thank Tobias Krojer and Jan Michael Peters for critical reading of the manuscript and helpful discussions. The IMP is funded by Boehringer Ingelheim, and this work was supported by an EU-ST5 Marie Curier Industry Host Fellowship (hpmi-ct-1999-00003) (K.K.) and BBSRC (M.E.).

Received: November 20, 2003
Revised: March 5, 2004
Accepted: March 8, 2004
Published: May 13, 2004

References

Ades, S.E., Connolly, L.E., Alba, B.M., and Gross, C.A. (1999). The Escherichia coli sigma(E)-dependent extracytoplasmic stress response is controlled by the regulated proteolysis of an anti-sigma factor. Genes Dev. *13*, 2449–2461.

Ades, S.E., Grigorova, I.L., and Gross, C.A. (2003). Regulation of the alternative sigma factor sigma(E) during initiation, adaptation, and shutoff of the extracytoplasmic heat shock response in Escherichia coli. J. Bacteriol. *185*, 2512–2519.

Alba, B.M., Leeds, J.A., Onufryk, C., Lu, C.Z., and Gross, C.A. (2002). DegS and YaeL participate sequentially in the cleavage of RseA to activate the sigma(E)-dependent extracytoplasmic stress response. Genes Dev. *16*, 2156–2168.

Alba, B.M., Zhong, H.J., Pelayo, J.C., and Gross, C.A. (2001). degS (hhoB) is an essential Escherichia coli gene whose indispensable function is to provide sigma (E) activity. Mol. Microbiol. *40*, 1323–1333.

Baldi, A., De Luca, A., Morini, M., Battista, T., Felsani, A., Baldi, F., Catricala, C., Amantea, A., Noonan, D.M., Albini, A., et al. (2002). The HtrA1 serine protease is down-regulated during human melanoma progression and represses growth of metastatic melanoma cells. Oncogene *21*, 6684–6688.

Bode, W., and Huber, R. (1976). Induction of the bovine trypsinogen-trypsin transition by peptides sequentially similar to the N-terminus of trypsin. FEBS Lett. *68*, 231–236.

Brunger, A.T., Adams, P.D., Clore, G.M., DeLano, W.L., Gros, P., Grosse-Kunstleve, R.W., Jiang, J.S., Kuszewski, J., Nilges, M., Pannu, N.S., et al. (1998). Crystallography & NMR system: A new software suite for macromolecular structure determination. Acta Crystallogr. D Biol. Crystallogr. *54*, 905–921.

Cabral, J.H.M., Petosa, C., Sutcliffe, M.J., Raza, S., Byron, O., Poy, F., Marfatia, S.M., Chishti, A.H., and Liddington, R.C. (1996). Crystal structure of a PDZ domain. Nature *382*, 649–652.

Campbell, E.A., Tupy, J.L., Gruber, T.M., Wang, S., Sharp, M.M., Gross, C.A., and Darst, S.A. (2003). Crystal structure of Escherichia coli sigmaE with the cytoplasmic domain of its anti-sigma RseA. Mol. Cell *11*, 1067–1078.

Clausen, T., Southan, C., and Ehrmann, M. (2002). The HtrA family of proteases: implications for protein composition and cell fate. Mol. Cell *10*, 443–455.

Collaborative Computational Project in Macromolecular Crystallography. (2002). High-throughput structure determination. Proceedings of the 2002 CCP4 study weekend. January, 2002. York, United Kingdom. Acta Crystallogr. D Biol. Crystallogr. *58*, 1897–1970.

De Las Penas, A., Connolly, L., and Gross, C.A. (1997). The sigmaE-mediated response to extracytoplasmic stress in Escherichia coli is transduced by RseA and RseB, two negative regulators of sigmaE. Mol. Microbiol. *24*, 373–385.

Doyle, D.A., Lee, A., Lewis, J., Kim, E., Sheng, M., and MacKinnon, R. (1996). Crystal structures of a complexed and peptide-free membrane protein-binding domain: Molecular basis of peptide recognition by PDZ. Cell *85*, 1067–1076.

Friedrich, R., Panizzi, P., Fuentes-Prior, P., Richter, K., Verhamme, I., Anderson, P.J., Kawabata, S., Huber, R., Bode, W., and Bock, P.E. (2003). Staphylocoagulase is a prototype for the mechanism of cofactor-induced zymogen activation. Nature *425*, 535–539.

Harris, B.Z., and Lim, W.A. (2001). Mechanism and role of PDZ domains in signaling complex assembly. J. Cell Sci. *114*, 3219–3231.

Harrison, S.C. (1996). Peptide-surface association: The case of PDZ and PTB domains. Cell *86*, 341–343.

Hegde, R., Srinivasula, S.M., Zhang, Z., Wassell, R., Mukattash, R., Cilenti, L., DuBois, G., Lazebnik, Y., Zervos, A.S., Fernandes-Alnemri, T., and Alnemri, E.S. (2002). Identification of Omi/HtrA2 as a mitochondrial apoptotic serine protease that disrupts inhibitor of apoptosis protein-caspase interaction. J. Biol. Chem. *277*, 432–438.

Hengge, R., and Bukau, B. (2003). Proteolysis in prokaryotes: protein quality control and regulatory principles. Mol. Microbiol. *49*, 1451–1462.

Huber, R., and Bode, W. (1978). Structural basis of the activation and action of trypsin. J. Mol. Biol. *11*, 114–122.

Jones, T.A., Zou, J.Y., Cowan, S.W., and Kjeldgaard, M. (1991). Improved methods For building protein models in electron-density maps and the location of errors in these models. Acta Crystallogr. A *47*, 110–119.

Jones, C.H., Dexter, P., Evans, A.K., Liu, C., Hultgren, S.J., and Hruby, D.E. (2002). Escherichia coli DegP protease cleaves between paired hydrophobic residues in a natural substrate: the PapA pilin. J. Bacteriol. *184*, 5762–5771.

Jones, J.M., Datta, P., Srinivasula, S.M., Ji, W., Gupta, S., Zhang, Z., Davies, E., Hajnoczky, G., Saunders, T.L., Van Keuren, M.L., et al. (2003). Loss of Omi mitochondrial protease activity causes the neuromuscular disorder of mnd2 mutant mice. Nature *425*, 721–727.

Kanehara, K., Ito, K., and Akiyama, Y. (2002). YaeL (EcfE) activates the sigma(E) pathway of stress response through a site-2 cleavage of anti-sigma(E), RseA. Genes Dev. *16*, 2147–2155.

Kim, D.Y., Kim, D.R., Ha, S.C., Lokanath, N.K., Lee, C.J., Hwang, H.Y., and Kim, K.K. (2003). Crystal structure of the protease domain of a heat-shock protein HtrA from Thermotoga maritima. J. Biol. Chem. *278*, 6543–6551.

Kraulis, P.J. (1991). Molscript - a program to produce both detailed and schematic plots of protein structures. J. Appl. Crystallogr. *24*, 946–950.

Krojer, T., Garrido-Franco, M., Huber, R., Ehrmann, M., and Clausen, T. (2002). Crystal structure of DegP (HtrA) reveals a new protease-chaperone machine. Nature *416*, 455–459.

Li, W., Srinivasula, S.M., Chai, J., Li, P., Wu, J.W., Zhang, Z., Alnemri, E.S., and Shi, Y. (2002). Structural insights into the pro-apoptotic function of mitochondrial serine protease HtrA2/Omi. Nat. Struct. Biol. *9*, 436–441.

Liao, D.I., Qian, J., Chisholm, D.A., Jordan, D.B., and Diner, B.A. (2000). Crystal structures of the photosystem II D1 C-terminal processing protease. Nat. Struct. Biol. *7*, 749–753.

Liberek, K., Galitski, T.P., Zylicz, M., and Georgopoulos, C. (1992). The DnaK chaperone modulates the heat shock response of Escherichia coli by binding to the sigma 32 transcription factor. Proc. Natl. Acad. Sci. USA *89*, 3516–3520.

Ma, Y., and Hendershot, L.M. (2001). The unfolding tale of the unfolded protein response. Cell *107*, 827–830.

Martins, L.M., Iaccarino, I., Tenev, T., Gschmeissner, S., Totty, N.F., Lemoine, N.R., Savopoulos, J., Gray, C.W., Creasy, C.L., Dingwall, C., and Downward, J. (2002). The serine protease Omi/HtrA2 regulates apoptosis by binding XIAP through a reaper-like motif. J. Biol. Chem. *277*, 439–444.

Martins, L.M., Turk, B.E., Cowling, V., Borg, A., Jarrell, E.T., Cantley, L.C., and Downward, J. (2003). Binding specificity and regulation of the serine protease and PDZ domains of HtrA2/Omi. J. Biol. Chem. *278*, 49417–49427.

Mecsas, J., Rouviere, P.E., Erickson, J.W., Donohue, T.J., and Gross, C.A. (1993). The activity of sigma E, an Escherichia coli heat-inducible sigma-factor, is modulated by expression of outer membrane proteins. Genes Dev. *7*, 2618–2628.

Merritt, E.A., and Bacon, D.J. (1997). Raster3D: Photorealistic molecular graphics. In Macromolecular Crystallography, Pt B, pp. 505–524.

Missiakas, D., Mayer, M.P., Lemaire, M., Georgopoulos, C., and Raina, S. (1997). Modulation of the Escherichia coli sigmaE (RpoE) heat-shock transcription-factor activity by the RseA, RseB and RseC proteins. Mol. Microbiol. *24*, 355–371.

Nie, G.Y., Li, Y., Minoura, H., Batten, L., Ooi, G.T., Findlay, J.K., and Salamonsen, L.A. (2003). A novel serine protease of the mammalian HtrA family is up-regulated in mouse uterus coinciding with placentation. Mol. Hum. Reprod. *9*, 279–290.

Otwinowski, Z., and Minor, W. (1997). Processing of X-ray diffraction data collected in oscillation mode. In Macromolecular Crystallography, Pt a, pp. 307–326.

Pallen, M.J., and Wren, B.W. (1997). The HtrA family of serine proteases. Mol. Microbiol. *26*, 209–221.

Perona, J.J., and Craik, C.S. (1995). Structural basis of substrate-specificity in the serine proteases. Protein Sci. *4*, 337–360.

Raivio, T.L., and Silhavy, T.J. (2001). Periplasmic stress and ECF sigma factors. Annu. Rev. Microbiol. *55*, 591–624.

Rouviere, P.E., De Las Penas, A., Mecsas, J., Lu, C.Z., Rudd, K.E., and Gross, C.A. (1995). rpoE, the gene encoding the second heat-shock sigma factor, sigma E, in Escherichia coli. EMBO J. *14*, 1032–1042.

Shridhar, V., Sen, A., Chien, J., Staub, J., Avula, R., Kovats, S., Lee, J., Lillie, J., and Smith, D.I. (2002). Identification of underexpressed genes in early- and late-stage primary ovarian tumors by suppression subtraction hybridization. Cancer Res. *62*, 262–270.

Songyang, Z., Fanning, A.S., Fu, C., Xu, J., Marfatia, S.M., Chishti, A.H., Crompton, A., Chan, A.C., Anderson, J.M., and Cantley, L.C. (1997). Recognition of unique carboxyl-terminal motifs by distinct PDZ domains. Science *275*, 73–77.

Srinivasula, S.M., Gupta, S., Datta, P., Zhang, Z., Hegde, R., Cheong, N., Fernandes-Alnemri, T., and Alnemri, E.S. (2003). Inhibitor of apoptosis proteins are substrates for the mitochondrial serine protease Omi/HtrA2. J. Biol. Chem. *278*, 31469–31472.

Straus, D., Walter, W., and Gross, C.A. (1990). DnaK, DnaJ, and GrpE heat shock proteins negatively regulate heat shock gene expression by controlling the synthesis and stability of sigma 32. Genes Dev. *4*, 2202–2209.

Walsh, N.P., Alba, B.M., Bose, B., Gross, C.A., and Sauer, R.T. (2003). OMP peptide signals initiate the envelope-stress response by activating DegS protease via relief of inhibition mediated by its PDZ domain. Cell *113*, 61–71.

Wickner, S., Maurizi, M.R., and Gottesman, S. (1999). Posttranslational quality control: Folding, refolding, and degrading proteins. Science *286*, 1888–1893.

Yamaguchi, H., Bhalla, K., and Wang, H.G. (2003). Bax plays a pivotal role in thapsigargin-induced apoptosis of human colon cancer HCT116 cells by controlling Smac/Diablo and Omi/HtrA2 release from mitochondria. Cancer Res. *63*, 1483–1489.

Yang, Q.H., Church-Hajduk, R., Ren, J., Newton, M.L., and Du, C. (2003). Omi/HtrA2 catalytic cleavage of inhibitor of apoptosis (IAP) irreversibly inactivates IAPs and facilitates caspase activity in apoptosis. Genes Dev. *17*, 1487–1496.

Young, J.C., and Hartl, F.U. (2003). A stress sensor for the bacterial periplasm. Cell *113*, 1–2.

Accession Numbers

The Protein Data Bank accession numbers for the nonactivated, the activated, and the hybrid forms of DegS are 1SOT, 1SOZ, and 1VCW, respectively.